Murphy, Damian J.; Alexander, Simon Peter; Vincent, Robert Alan
Interhemispheric dynamical coupling to the southern mesosphere and lower thermosphere,
Journal of Geophysical Research, 2012; 117:D08114.

Interhemispheric dynamical coupling to the southern mesosphere and lower thermosphere

D. J. Murphy,[1] S. P. Alexander,[1] and R. A. Vincent[2]

Received 12 September 2011; revised 4 March 2012; accepted 21 March 2012; published 28 April 2012.

[1] Wind observations obtained between 1995 and 2011 using the MF radar at Davis have been used to demonstrate the modifying role the quasi-biennial oscillation (QBO) plays on some aspects of interhemispheric coupling identified by previous authors. The response of the meridional wind in the southern summer polar MLT to changes in winter stratospheric planetary wave activity is shown to change sign according to the phase of the QBO. The time delay associated with the coupling is also shown to vary with QBO phase, with an eastward QBO providing a more rapid response. Coupling to the MLT meridional winds is strongest in January. Parts of the mechanism currently proposed have been tested using UKMO assimilated observations. The signatures of some aspects of this mechanism are present in the data. However, some differences to the mechanism are also apparent, in particular the effectiveness of the mechanism near the equator. An explanation for the QBO modulation of the MLT wind response to interhemispheric coupling is proposed on the basis of these differences.

Citation: Murphy, D. J., S. P. Alexander, and R. A. Vincent (2012), Interhemispheric dynamical coupling to the southern mesosphere and lower thermosphere, *J. Geophys. Res.*, *117*, D08114, doi:10.1029/2011JD016865.

1. Introduction

[2] The middle atmosphere's pole-to-pole residual circulation explains observed characteristics such as the cold summer mesopause [e.g., *Andrews et al.*, 1987] and is supported by theoretical and modeling studies [*Dunkerton*, 1978; *Lindzen*, 1981; *Geller*, 1983]. But direct measurements of the associated zonal-mean meridional and vertical velocities are made difficult by the large spatial and temporal variability of middle atmosphere winds. As a result, the exact nature of the residual circulation and the processes responsible have not been extensively explored in observations.

[3] A surprising relationship between the state of the winter stratosphere and the summer mesopause has now been identified and has the potential to inform our understanding of the residual meridional circulation. The 2002 MACWAVE/MIDAS program of radar and rocket observations of wind and temperature in the northern high-latitude mesosphere [*Becker et al.*, 2004], which were made in the lead up to the first recorded southern hemisphere stratospheric warming [e.g., *Baldwin et al.*, 2003], were found to differ somewhat from the climatological average [*Becker et al.*, 2004; *Becker and Fritts*, 2006, and references therein]. These data provided the catalyst for modeling [*Becker and Fritts*, 2006; *Karlsson et al.*, 2009a; *Körnich and Becker*, 2010] and observational [*Karlsson et al.*, 2007, 2009b; *Espy et al.*, 2011] studies of this form of interhemispheric coupling.

[4] Thus, a rare southern hemisphere planetary wave event was seen to elicit a northern hemisphere response. Noting that stratospheric planetary waves have larger amplitudes in the northern hemisphere than in the south, it is clear that southern hemisphere observations are valuable in the context of interhemispheric coupling studies: greater variability in the source of the coupling should provide greater variability in the response. A medium frequency (MF) radar situated at Davis station (68.6°S, 78.0°E) has been operating since 1993 and so can provide a long term data set in which to identify responses in the mesosphere and lower thermosphere (MLT). The United Kingdom Met Office (UKMO) assimilated data set (R. Swinbank et al., Stratospheric assimilated data, British Atmospheric Data Centre, 2006, http://badc.nerc.ac.uk/data/assim/) (hereinafter Swinbank et al., online data, 2006) can provide concurrent information on the global troposphere, stratosphere and lower mesosphere. In this paper, these data sets are combined to study interhemispheric coupling between the stratosphere and the mesosphere. The results of the analysis are presented in the next section. The currently proposed mechanism [see *Karlsson et al.*, 2009a; *Körnich and Becker*, 2010, and references therein], is then described and provides a reference for the interpretation of our findings. Some notes on the relationship between zonal-mean meridional and

[1]Australian Antarctic Division, Department of Sustainability, Environment, Water, Population and Communities, Kingston, Tasmania, Australia.
[2]Department of Physics and Mathematical Physics, University of Adelaide, Adelaide, South Australia, Australia.

Corresponding Author: D. J. Murphy, Australian Antarctic Division, Department of Sustainability, Environment, Water, Population and Communities, 203 Channel Hwy., Kingston, Tas 7050, Australia. (damian.murphy@aad.gov.au)

0148-0227/12/2011JD016865

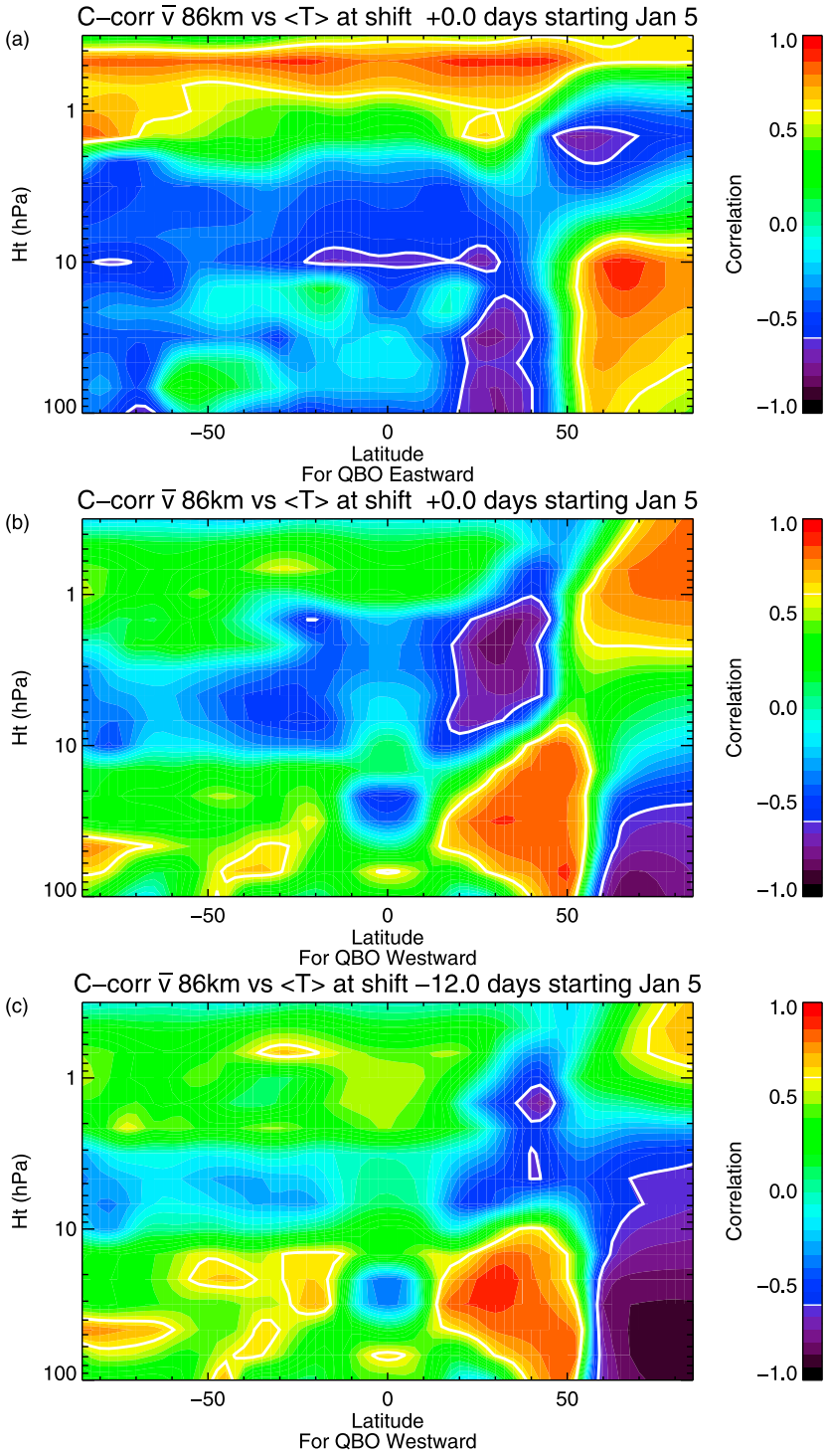

Figure 1. Correlation of the average Davis meridional wind from January 5 at 86 km with the zonal-mean temperature from 100–0.3 hPa for (a) QBO eastward and (b) westward. (c) The QBO westward case for a lag of −12 days.

vertical velocity, which inform this interpretation, have been included in the appendix.

2. Analysis and Results

[5] In the observational and modeling studies described above, noctilucent cloud (NLC) characteristics or temperature near the mesopause were used as the summer hemisphere correlant. For this study, it was necessary to choose parameters that can be obtained from an MF radar. The Davis MF radar operates at a frequency of 1.94 MHz and receives radar echoes from between 70 to 110 km although those between 80 and 94 km are considered most reliable for wind

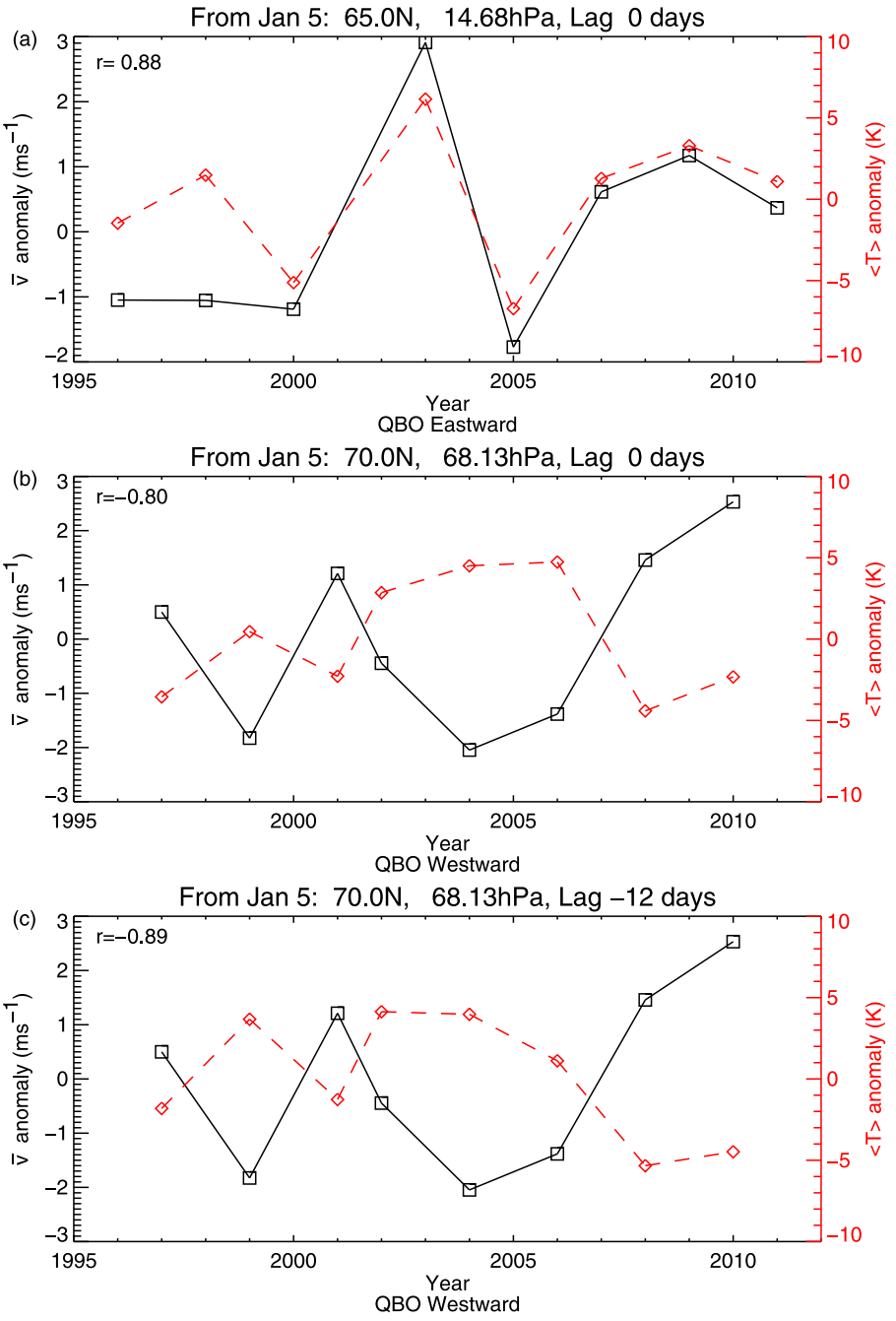

Figure 2. Time series of MF radar wind and stratospheric zonal mean temperature anomalies for (a) QBO eastward at 65.0°N, 14.68 hPa and (b) QBO westward at 70.0°N, 68.13 hPa. (c) The QBO westward case for a lag of −12 days. The correlation coefficient for each case is also shown.

determinations. Data are sampled every 2 km, however, due to pulse length considerations, adjacent height samples are not independent (a ≥ 4 km height spacing provides independent wind determinations). Further information on the radar is included in *Murphy et al.* [2007].

[6] The mean meridional velocity was preferred to the zonal velocity because the former is coupled to the vertical wind (and thus temperature) through some terms of the continuity equation (see Appendix A). (The vertical velocity obtained from MF radars is not considered reliable because of the potential for folding of large horizontal winds onto the small vertical component [*Murphy*, 1984].) The meridional velocity in the MLT is also less coupled to its value at other heights than the zonal velocity; the processes forcing the meridional wind tend to be more localized in height. This makes it more likely that any correlations identified are associated with effects on the MLT meridional wind itself.

[7] It is noted that the observations made from Davis are local to the sampling volume of the radar and thus are not zonal-mean values. Previous studies using noctilucent

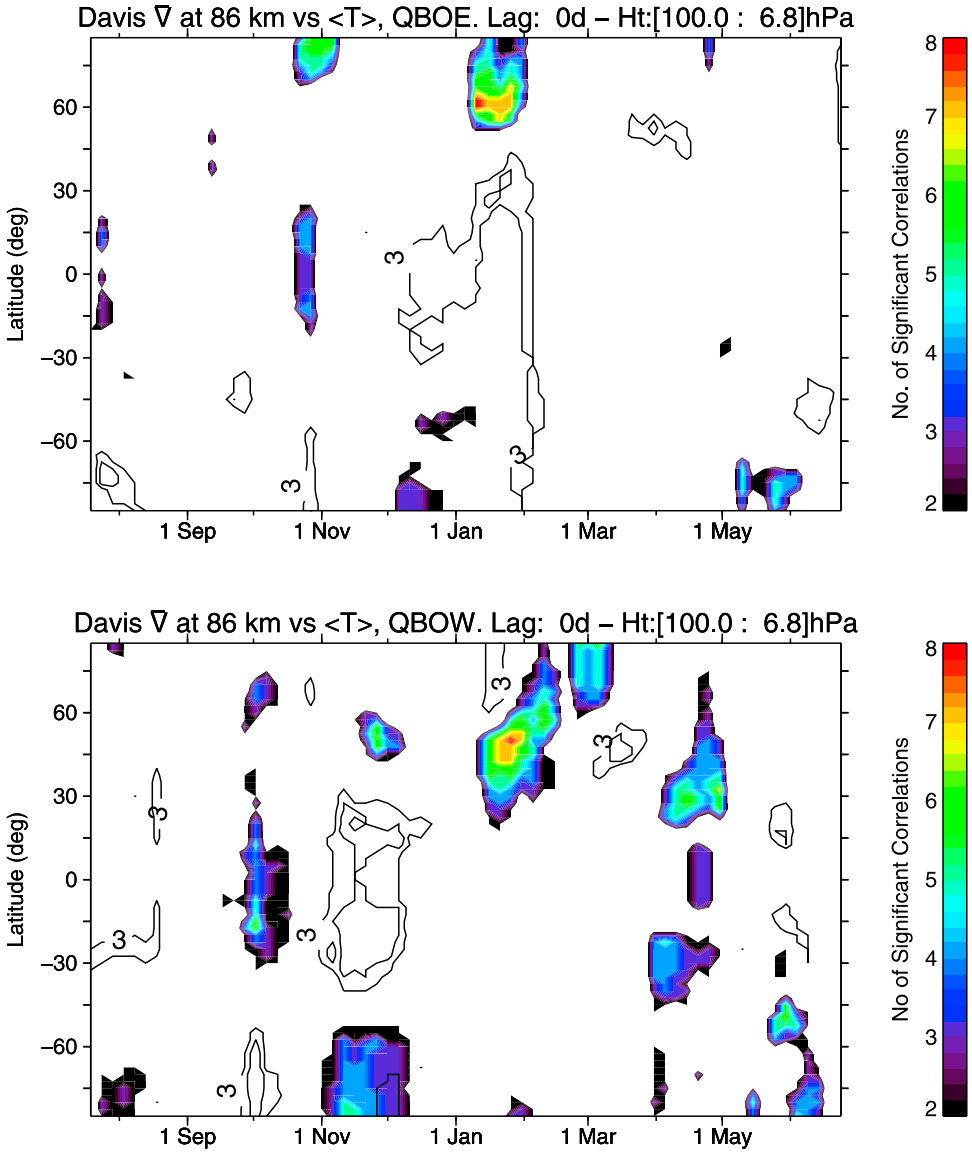

Figure 3. Significant correlation occurrence rates over height range 100–6.8 hPa for QBO (top) eastward and (bottom) westward. Positive correlations are indicated by color, negative correlations at levels of 3 and 5 are contoured.

clouds have used a longitudinal average to obtain their parameters. Arguments that relate meridional velocity to vertical velocity also use zonal-mean quantities [e.g., *McIntyre*, 1989]. It is therefore necessary to extract a parameter from the Davis winds that approximates the zonal mean. After assuming that short- and long-period propagating waves are the source of variation from the zonal mean, the winds are averaged in time to remove their effect. Although most planetary waves are expected to be weak in the summer polar MLT, the quasi two-day wave can be large in January–February [*Murphy et al.*, 2007]. Thus, an averaging window of 30 days is applied. This averaging reduces wind measurements to a single parameter for further analysis.

[8] Previous studies successfully used the zonal-mean stratospheric temperature as the global correlant [*Karlsson et al.*, 2007, 2009a]. Although a temperature variation is not thought to trigger the coupling mechanism [*Körnich and Becker*, 2010], temperature responds to the vertical motions associated with planetary-wave driven meridional circulations in the stratosphere and is thus a good measure of the integrated planetary wave activity [*Becker and Schmitz*, 2003]. For this reason, the zonal-mean temperature throughout the domain of the UKMO stratospheric assimilated data set is used as the second correlant in this study.

[9] The analysis used here begins by defining 30-day windows (as noted above) starting from a given day of each year in the multiyear data set. The radar winds at Davis and the zonal-mean UKMO temperature at each latitude and height within the windows are averaged to form a collection of time series. Climatological averages (calculated using the same windows) are then removed from each time series. The Pearson correlation coefficient is calculated for each time

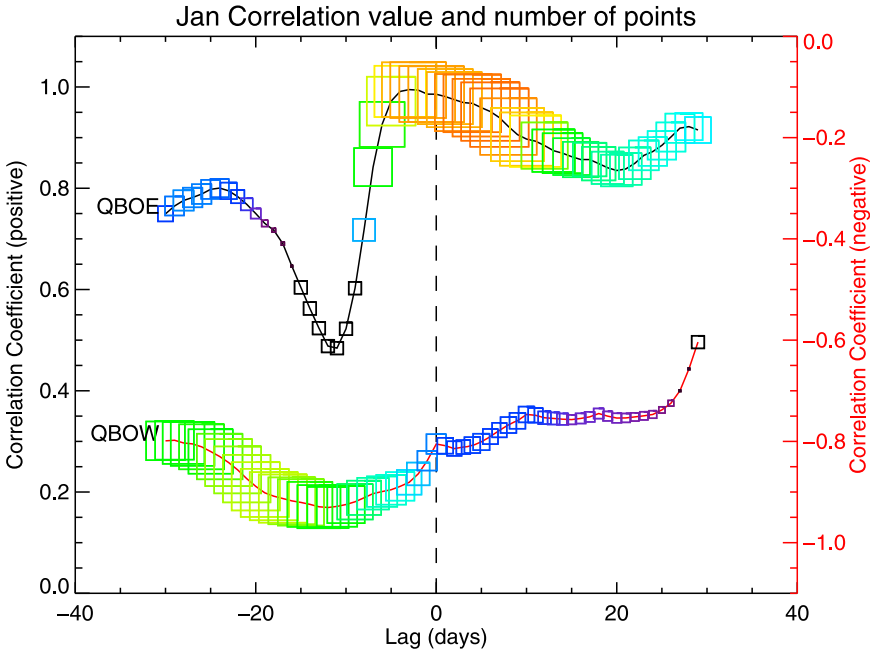

Figure 4. Maximum (black line and axis) and minimum (red line and axis) correlation coefficients in the northern lower stratosphere for lags in the range ±30 days. Squares indicate the number of significant correlation points. Maximum correlation values are drawn from the QBO eastward case and minima from the QBO westward case.

series, yielding a latitude-height grid of the correlation. The analysis is applied over an interval where consistent assimilation parameters are used in the UKMO data which extends from late 1995 to 2011 (16 southern summers in total). One of the windows used to extract the time series can be shifted to allow the computation to be carried out at non-zero lag.

[10] Planetary waves in the winter stratosphere are thought to play a significant role in the interhemispheric coupling [e.g., *Karlsson et al.*, 2009a]. The Quasi-Biennial Oscillation (QBO) [see, e.g., *Baldwin et al.*, 2001] is a significant modulator of planetary wave activity in the winter hemisphere and so could play a role in the interhemispheric coupling being investigated here. The long duration of the Davis MF radar data set makes it possible to sort our observations according to the phase of the QBO and retain significance in our correlations. For this work, the QBO phase is determined by zonally averaging the zonal wind at a (UKMO output) height of 46.4 hPa above the equator using the same 30-day averaging windows applied to the other parts of this analysis.

[11] The results of this analysis as applied to 86 km wind data within a 30 day window starting January 5 are presented in Figure 1. For this analysis, there is one data point per year for each latitude and height. No relative time shift (lag) has been applied to the data windows in the upper two panels. The height at which Davis winds are measured is above the upper limit of the UKMO data (and of this plot), so local correlations cannot be calculated. Regions where the correlation coefficient is significant to the 90% level (two-sided) are shown within white lines. Figure 1a shows the correlation for those cases when the wind in the equatorial stratosphere at 46 hPa is eastward (hereafter QBO eastward) whereas Figure 1b is for QBO westward. Regions of significant correlation exist in the northern lower stratosphere in both panels (although, as discussed later, the signs of these correlations vary with QBO phase). This analysis was also applied to the observations with no sorting with respect to QBO phase (not shown). Despite the lower absolute correlation required for significance (due to the higher number of data points), the regions of significant correlation were less extensive than when the QBO phases were separated.

[12] To ensure that the winter hemisphere correlation patterns presented in Figure 1 are not fortuitous, the analysis has been run using three consecutive 10-day data windows from January 5. Although the regions of significant correlation decrease in size (presumably due to a decrease in the statistical reliability of the radar winds or the influence of planetary wave period variations on the stratospheric temperature averages), their pattern remains consistent with those shown in Figures 1a and 1b. The analysis has also been run using MF radar meridional winds at 92 km. As noted above, these wind determinations are independent of those at 86 km. The structure of the correlation patterns exhibited for 92 km (not shown) are similar to that for 86 km but with smaller significance regions.

[13] Pairs of time series of the wind and temperature anomaly data contributing to the strong correlation regions in the high latitude stratosphere shown in Figure 1 (65°N, 14.68 hPa for QBO eastward; 70°N, 68.13 hPa for QBO Westward) are presented in Figure 2. Only the years for the corresponding QBO phase are included in each panel, providing 8 data points per time series in both cases. The strong

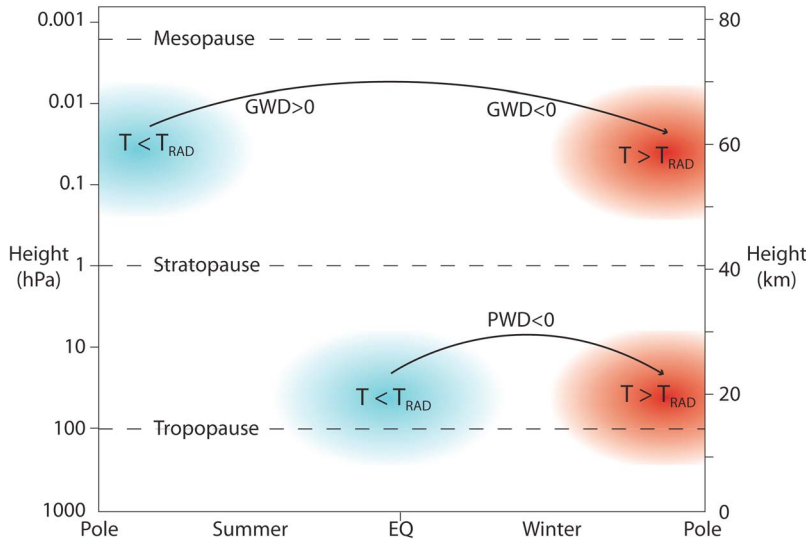

Figure 5. The background dynamical state of the middle atmosphere at solstice [after *Körnich and Becker*, 2010].

correlation and anticorrelation suggested by the coefficients in Figure 1 are clearly shown in these data.

[14] The seasonal variations of the correlations are shown in Figure 3 where the number of significant positive correlation values between the heights of 100 and 6.8 hPa (inclusive) are imaged as a function of latitude and season. This height range is chosen to capture the high correlation regions shown in Figure 1. Negative but significant correlations are included with black contours. It can be seen that positive correlations are most common in the northern hemisphere during January with the peak occurrence falling in mid to late January. Adjacent negative correlations are also present at this time. These latitudinally adjacent correlation features are consistent with the proposed mechanism for interhemispheric coupling. For the remainder of this paper, analysis will therefore be focused on a 30-day window centered on the peak in Figure 3 (i.e. starting on January 5).

[15] The lags at which the correlations maximize are investigated through Figure 4. Here a 15-day analysis window is used as a compromise between potential planetary wave contamination and the resolution of the variations in lag being investigated. The radar data window is centered on the latter half of January (15 days from January 16th) to remain consistent with Figure 3. The black line in Figure 4 describes the maximum correlation in the northern hemisphere between pressure levels of 100 and 6.8 hPa (inclusive). The size (and color) of the boxes superimposed on the line are proportional to the number of significant correlations in that region. It can be seen that large correlations and areas of significance occur close to zero lag for the QBO eastward case. (Recall that these positive correlations occur near the pole.)

[16] The red line in Figure 4 describes the minimum (maximum negative) correlation in the same region for the QBO westward case (with reference to the right hand axis). The minimum correlation and largest correlation areas do not occur near zero lag in this case with the minimum correlation being near a lag of −12 days. The correlation as a function of latitude and height for this lag is presented in Figure 1c. It can be seen that the stronger correlations in the lower stratosphere are accompanied by weaker and smaller correlations higher up (cf. Figure 1b). These differences in correlation between the QBO eastward and westward cases suggest differences in the interhemispheric coupling mechanism. These are discussed further in a later section.

[17] Figure 1 shows that variations in the MLT meridional wind above Davis are associated with variations in the zonal-mean temperature in the Northern high-latitude stratosphere. A southern hemisphere interhemispheric response in the MLT meridional wind can be added to the wind, temperature and NLC responses already identified by *Becker et al.* [2004], *Karlsson et al.* [2007] and *Espy et al.* [2011].

3. A Mechanism for Interhemispheric Coupling

[18] A mechanism has been proposed by *Becker and Fritts* [2006] that explains the coupling identified in *Becker and Fritts* [2006] and *Karlsson et al.* [2007, 2009b]. Further modeling work by *Karlsson et al.* [2009a] has improved our understanding of this mechanism and it provides a useful reference for comparison with observations. *Körnich and Becker* [2010] describe this mechanism in three stages and these will be presented as a prelude to discussions of the observations made here. For brevity, the proposed mechanism will be termed the BKK mechanism, recognizing the lead authors listed above.

[19] The mean dynamical state of the middle atmosphere is described in Figure 5. Planetary wave breaking in the winter stratosphere applies a westward (negative) drag on the atmosphere and forces a residual circulation from the equator to the pole (often termed the Brewer-Dobson circulation). Upwelling near the equator associated with this circulation cools the tropical tropopause relative to its radiative equilibrium temperature T_{rad}. The downwelling at the polar end of this circulation has the opposite effect; the tropopause

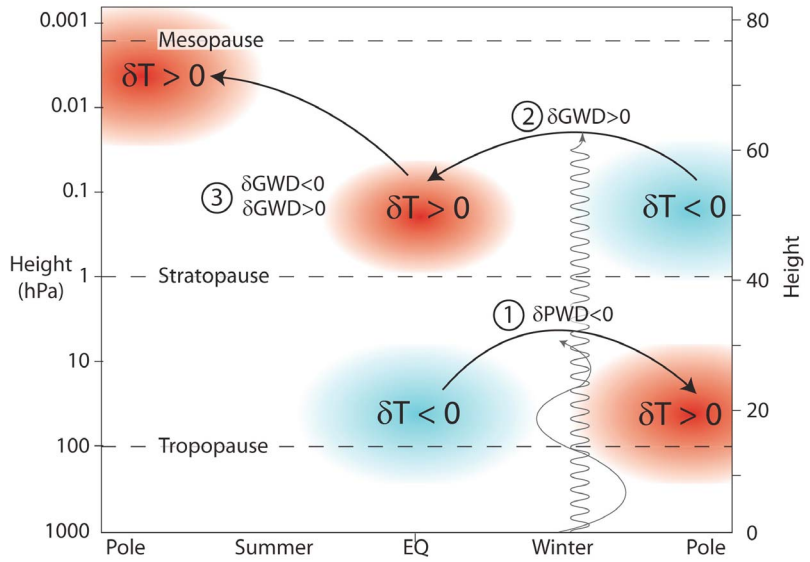

Figure 6. Three stages of the effect of a perturbation to the background dynamical state of the middle atmosphere at solstice [after *Körnich and Becker*, 2010].

and lower stratosphere are warmed relative to their radiative equilibrium temperature. In the mesosphere, the action of breaking gravity waves, whose phase speed spectrum is filtered as they propagate through the stratosphere, provides a zonal drag that is positive in the summer hemisphere and negative in the winter hemisphere [*Lindzen*, 1981]. The balance of these drags with the Coriolis force in each hemisphere drives a residual circulation that flows from the summer to the winter pole around the mesopause. The upwelling near the summer pole has an intense cooling effect leading to temperatures below the radiative equilibrium value and the observed cold summer mesopause. The winter mesosphere is warmed by the downwelling part of this pole-to-pole circulation.

[20] The trigger for the BKK coupling mechanism is a change to the planetary wave activity in the winter stratosphere (see Figure 6). Here, the consequences of an increase in this activity are described but it is noted that the reverse is thought to apply equally [*Körnich and Becker*, 2010; *Karlsson et al.*, 2009a].

[21] *Stage 1* invokes an increase in winter stratospheric wave activity, which causes a decrease in the planetary wave drag such that it is more strongly (negative) westward. This has the effect of enhancing the stratospheric residual circulation, warming the cold winter polar tropopause and cooling the warm equatorial stratosphere. The resultant decrease in the meridional temperature gradient decreases the strength of the zonal winds in the winter lower stratosphere.

[22] In *Stage 2*, the gravity-wave drag applied above the stratopause is affected by the change in the winter stratospheric zonal wind and its associated gravity-wave filtering. Without perturbation, it is expected that only large positive zonal phase speed gravity waves will accompany the negative phase speed waves that propagate into the winter mesosphere. Under perturbed conditions, more positive phase speed waves are transmitted through the stratosphere and the negative phase speed waves break at lower heights [see *Körnich and Becker*, 2010, Figure 2]. As a result, a less negative gravity-wave drag is present in the mesosphere. The background gravity-wave drag in this region is of the opposite sign so this perturbation acts to weaken the mesospheric circulation in the winter hemisphere. Thus, for the enhanced stratospheric planetary wave activity described in stage 1, the lower mesosphere is expected to warm near the equator and the polar winter lower mesosphere cools [*Körnich and Becker*, 2010].

[23] In *Stage 3*, the effect of the warm tropical mesosphere is propagated from near the equator to the summer mesosphere. *Körnich and Becker* [2010] and *Karlsson et al.* [2009a] describe a feedback process whereby the anomalously warm equatorial lower mesosphere creates a vertical gradient in gravity wave drag on its summer poleward side. This then creates a warm anomaly and the feedback continues. As a result, the tropical temperature anomaly propagates poleward and upward to the summer polar mesosphere (as described in Figure 6).

[24] As noted above, the proposed mechanism can be applied to a weakening of the planetary wave drag to yield a cooling of the summer polar mesosphere. In the following section, the mechanism described above is considered in the light of the observations used in this analysis.

4. Discussion

[25] The results in Figure 1 show differing forms of correlation for the two phases of the QBO. The winter planetary-wavefield, whose perturbation is thought to launch the interhemispheric coupling, is modulated by the QBO [e.g., *Baldwin et al.*, 2001]. The latitudinal extent of the winter-time eastward winds is also altered somewhat by the QBO, with the potential for changes to the gravity-wave filtering near the equator. In this section, the potential role of the QBO as a modulator of interhemispheric coupling is considered for each QBO phase. This is done in the context of

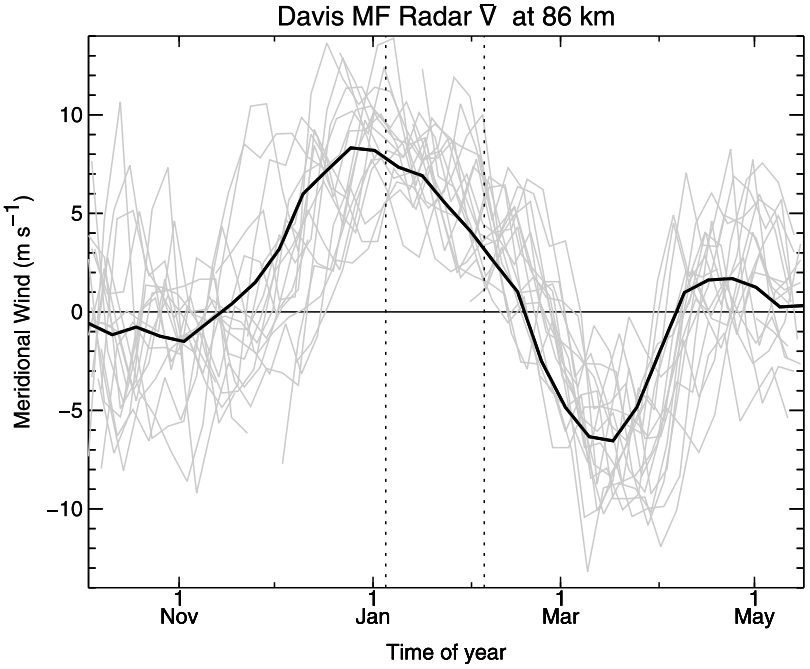

Figure 7. Variations in the daily averaged Davis meridional wind at 86 km around the summer for duration of this analysis. The thick solid line is a running mean.

the meridional velocity observations presented in this paper and the BKK mechanism summarized above.

[26] A recent paper by *Espy et al.* [2011] identified a variation in the temperature of the atmosphere near 87 km above Sweden (at 57.4°N and 59.5°N) in July that correlates with July temperatures in the southern hemisphere stratosphere (40°–60°S near 50 hPa) and is anticorrelated with the equatorial wind near 50 hPa (a QBO indicator). Strong evidence for a signature of the QBO in their temperature measurements is provided. They note that the Holton-Tan effect [*Holton and Tan*, 1980] explains the QBO modulation of the southern stratospheric temperature. Unlike the current study, *Espy et al.* [2011] do not apply separate correlation analyses to each phase of the QBO, and thus do not identify changes in the nature of the interhemispheric coupling mechanism with QBO state: the results of *Espy et al.* [2011] can be explained by a BKK mechanism coupling Holton-Tan induced QBO variations of the July stratospheric temperature to the northern mesopause.

4.1. Meridional Velocity

[27] Figure 1 presents two zero-lag correlations between global zonal-mean temperatures and 30-day averages of the Davis meridional winds starting January 5 at 86 km. However, in Figure 1a, only those 30-day windows that correspond to eastward winds above the equator are included. It can be seen that for this phase of the QBO, a region of high positive correlation is present poleward of 50°N between ∼68 and ∼6.8 hPa. The larger values of correlation are near the upper end of this height range. A smaller region of significant anticorrelation is present over a smaller height range in the winter subtropics. The correlations for westward QBO phase presented in Figure 1b are opposite to the QBO eastward case: the high-latitude lower stratosphere contains a region of significant anticorrelation with the larger correlation magnitudes in the lower part of this region. The region of anticorrelation is larger and its coefficient is of larger magnitude at a lag of −12 days as shown in Figure 1c.

[28] Thus, the summer mesosphere above Davis responds with meridional velocities at 86 km that are more positive when the winter polar lower stratosphere is warmer for an eastward phase of the QBO. When the QBO is in its westward phase, the meridional velocities become more negative for the same winter polar lower stratosphere perturbations.

[29] The analyses carried out by *Karlsson et al.* [2007, 2009a, 2009b] focused on the temperature response in the mesosphere or NLC characteristics that are affected by temperature. In the present study, temperature is not available and meridional velocity is used as a correlant. Intuitive arguments suggest a relationship between the zonal-mean vertical velocity $\overline{w}$ (which has a potentially strong adiabatic heating or cooling effect associated with it) and the zonal-mean meridional velocity $\overline{v}$. This relationship is discussed in Appendix A and it is shown that, although $\overline{v}$ is not strictly proportional to $\overline{w}$, in the southern hemisphere, positive $\overline{v}$ is likely associated with positive $\overline{w}$ and *vice versa*.

[30] Observations support this view. Daily averaged Davis meridional winds at a height of 86 km are presented in Figure 7 for the summer months. Each grey line represents a single year with the darker line a 15-day running mean of the data. It can be seen that all the meridional wind values for January are positive at this height. Both QBO phases are present in this diagram so it is clear that the meridional velocity is positive during January in both cases. The vertical velocity is not known but the cold summer mesopause, whose altitude is close to the 86 km level considered here, suggests upward mean vertical velocities.

[31] It should be noted, however, that the vertical gradient of vertical velocity also plays a role in the relationship between $\overline{v}$ and $\overline{w}$. Combining the zonal-mean version of the continuity equation with the hydrostatic equation and assuming that the high-latitude zonal-mean meridional velocity varies linearly with latitude from a zero at the pole, it is possible to show that, at a given height z,

$$\overline{v} \propto \frac{\overline{w}}{H} - \frac{\partial \overline{w}}{\partial z}, \tag{1}$$

where H is the density scale height (see Appendix A).

[32] In the context of the observations presented in this paper, the above expression allows a difference in the temperature and meridional wind responses in the polar MLT that is not present if $\overline{v} \propto \overline{w}$. The differential form of equation (1),

$$\delta\overline{v} \propto \delta\left(\frac{\overline{w}}{H}\right) - \delta\left(\frac{\partial \overline{w}}{\partial z}\right), \tag{2}$$

shows that a perturbation in meridional velocity can be related to a change in vertical velocity or in its vertical gradient. Temperature variations, which will be more strongly coupled to the vertical velocity than to its gradient, can also be weakly coupled to $\overline{v}$ variations. This is consistent with CMAM model observations (B. Karlsson, personal communication, 2010) that show January meridional velocities correlated with temperatures at the latitude of Davis and at 84 km with a coefficient of ~ -0.4. This also suggests the characteristics of coupling to the meridional wind shown here (and the way they change with QBO state) could differ to those seen in temperature and temperature-related parameters used in other studies.

4.2. The Role of the QBO in Interhemispheric Coupling

[33] The UKMO assimilated data set (Swinbank et al., online data, 2006) can be used to consider stages of the BKK mechanism described in section 3. It is noted that this data set is subject to limitations in both the coverage of the observations it ingests (particularly in the early years used in this study) and the assimilation model's workings near its upper boundary. These could affect the quality of the data in the upper stratosphere and lower mesosphere, and the inferences drawn from them. However, the differences in response across QBO phase (without change in the limitations of the assimilation) and the extension of some of the features described below to lower altitudes, attest to the utility (with caution) of using the UKMO data to study aspects of the mechanism proposed for interhemispheric coupling.

[34] In the first stage of the proposed coupling, increased (decreased) planetary-wave drag leads to a warmer (colder) polar stratosphere due to stronger (weaker) downwelling (see Figure 6). Stronger (weaker) upwelling near the equator is also proposed. This latter relationship is tested by correlating the zonal-mean temperature (a proxy for planetary wave activity [*Becker and Schmitz*, 2003]) over 30 days from January 5 between 100–32 hPa at high northern latitudes with the corresponding global zonal-mean temperature (above 100 hPa), and the result is shown in Figure 8. The differing responses for the two phases of the QBO (as depicted in Figure 1) influence the selection of latitudes and height ranges used to correlate with global temperatures: for the QBO Eastward case, a region near 60°N from 100–68 hPa is used, whereas, for the QBO westward case, a region near 70°N and 68–32 hPa is chosen. Both of these regions are near the base heights of the correlations seen in Figure 1 to take advantage of the accumulated effect of the downwelling that is present in the polar stratosphere at this time of year. Figure 8a describes the QBO eastward case and it can be seen that warm (cold) temperatures in the lower polar stratosphere are associated with warm (cold) polar temperatures up to around 10 hPa, and with cold (warm) temperatures at mid latitudes.

[35] In the QBO Westward case (Figure 8b), the midlatitude lower stratospheric anticorrelation region remains significant to lower latitudes although the high anticorrelation values tend to coincide with those for QBO Eastward. Notably, the midlatitude region of positive correlation near 1 hPa is stronger and more extensive in the QBO Westward case. Although the exact form of this pattern varies with the height and latitude chosen for the first correlant within the polar (>60°N) lower stratosphere, these patterns largely persist (for both phases of the QBO).

[36] Model investigations of the proposed interhemispheric coupling mechanism have been carried out [*Karlsson et al.*, 2009a; *Körnich and Becker*, 2010]. In the former, the Canadian Middle Atmosphere Model (CMAM) provided data for a composite analysis that compared the atmospheric response to strong and weak planetary wave activity. This allowed both the genesis of the coupling and the spatial distribution of the associated anomalies to be investigated. It should be noted, however, that the CMAM model as used in that study does not include a QBO.

[37] Height-latitude maps of the temperature perturbation associated with anomalously strong planetary-wave activity are shown in *Karlsson et al.* [2009a, Figure 6]. Once the impacts of the planetary wave perturbations are established (after a lag of around 10 days), a pattern similar to that described in *Körnich and Becker* [2010] is apparent with a warm polar and a cold equatorial stratosphere. The upper limit of these anomalies is near 1 hPa and so is higher in the model than in the UKMO data presented here in Figure 8. However, the observations presented in this paper are for January; the composites presented in *Karlsson et al.* [2009a] are for strong (or weak) planetary wave events whenever they occur during local winter and are consistent with observations during a stratospheric warming [*Randel*, 1993]. The contributions of the planetary-wave drag anomaly relative to the effect of gravity-wave drag could also affect the modeled vertical distribution of the correlation pattern. (This in turn is dependent on the gravity wave source, propagation and decay characteristics used in the model; something that is often poorly constrained by observations.) In general though, there is good agreement between the predicted, modeled and observed (here) characteristics of the lower stratosphere temperature response to changed planetary wave activity. Away from the equator, the stage 1 response is similar for QBO eastward and westward.

[38] In the second stage of the BKK mechanism, *Körnich and Becker* [2010] note that the change in the stratospheric planetary wavefield that influenced the temperature in stage one, alters the filtering of gravity waves as they propagate upward toward the mesosphere. On breaking, these gravity waves alter the meridional circulation responsible for the cold

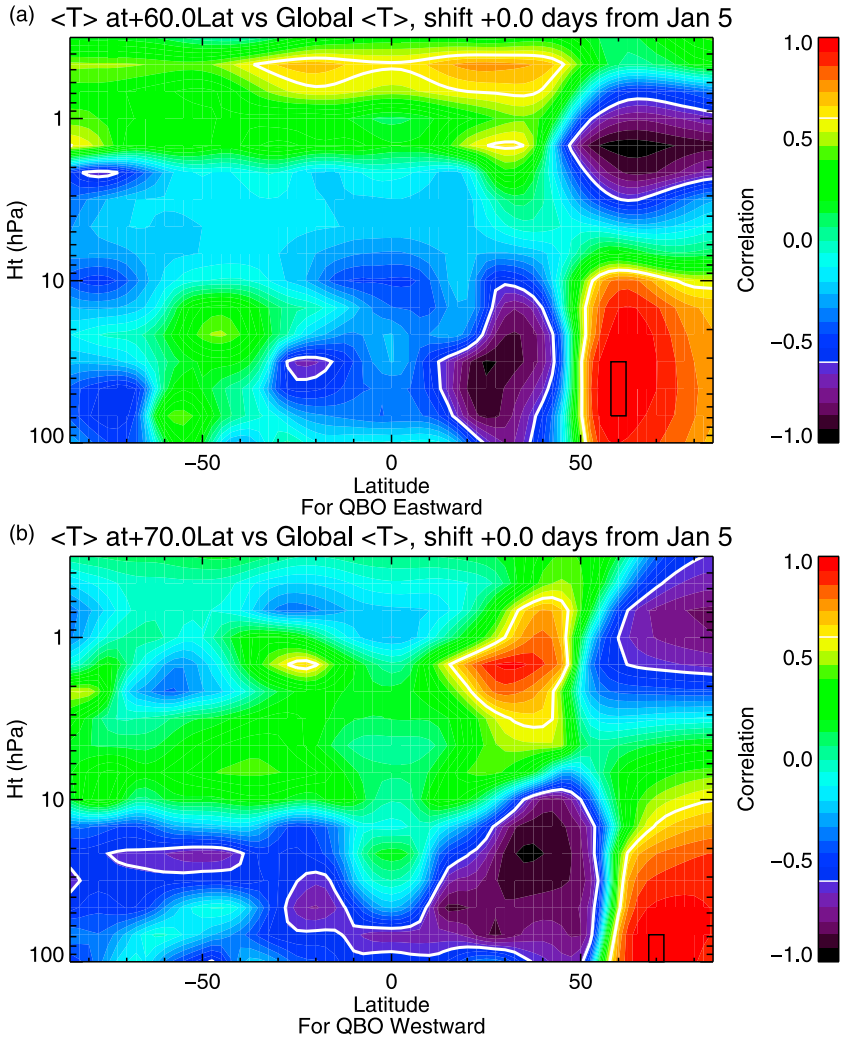

Figure 8. Correlation of the average zonal mean temperature at (a) 60°N between 68–32 hPa (indicated by a box) during QBO eastward and (b) 70°N between 100–68 hPa during QBO westward, with the global zonal-mean temperature from 100–0.3 hPa.

summer and warm winter polar mesospheres. The usual negative (westward) drag is said to be weakened by enhancements to the stratospheric planetary wave drag such that a cold anomaly appears in the polar mesosphere and a warm anomaly is created in the tropical mesosphere (see Figure 6).

[39] Inspection of the higher altitude results in Figure 8 show that the response in the UKMO data differs from the proposed mechanism. A region of significant anticorrelation in the high latitudes near 1 hPa suggests the polar part of the proposed temperature perturbation is present in both QBO phases. The QBO eastward case is lower than the QBO westward and is significant to a lower latitude. The vertical separation between the polar correlation regions is greater for QBO westward. Importantly, the region of positive correlation at midlatitudes between 1–2 hPa in the QBO westward case is absent in the QBO eastward case. (It is not known whether the region of positive correlation near 0.5 hPa at midlatitudes is real; suspicions arise due to its proximity to the top of the UKMO data domain.) These characteristics remain out to lags of ±5 days.

4.3. Propagation of Coupling From Equator to Summer Pole

[40] In the previous section, it was shown that the mid-to-low latitude temperature response near 1 hPa associated with the BKK interhemispheric coupling mechanism is different for the two phases of the QBO in the UKMO data. This is the region associated with stage 2 of the BKK mechanism and is the launching point for its stage 3. There is also some difference between these observations and the predictions of *Körnich and Becker* [2010] of the response near the equator. The observations in Figures 1 and 8 show almost no significant response at the equator (a small region near the base of Figure 8b being the exception). This is in contrast to Figure 6 [after *Körnich and Becker*, 2010], where an equatorial response in the lower stratosphere and lower mesosphere is predicted.

[41] The lack of equatorial response in the observed temperature can be understood after recalling the proposed sequence of events leading to a temperature perturbation. A change in the zonal-mean zonal drag (here due to gravity

waves) causes a change in the zonal-mean meridional circulation which, through the requirements of continuity (see Appendix A), causes a change in the zonal-mean vertical wind. The adiabatic heating or cooling effect of this vertical wind then leads to a change in the temperature. The meridional response to a zonal drag is necessary to balance the Coriolis force, whose magnitude is a function of latitude [see, e.g., *Andrews et al.*, 1987]. However, near the equator, the Coriolis effect is absent or weak, as too is the meridional response to a zonal force. It follows, then, that the temperature response due to changes in gravity wave drag (stage 2 of the BKK mechanism) would also be negligible near the equator. (It is noteworthy that the strength of the Coriolis effect at high latitudes, combined with a stronger relationship between meridional and vertical velocity there can also explain the strong temperature response to zonal-drag changes near the poles).

[42] Inspection of the CMAM model results suggests there is an equatorial response to the gravity-wave drag anomaly; a temperature anomaly like that predicted by the BKK mechanism is present in the winter mesosphere [*Karlsson et al.*, 2009a, Figure 6]. However, the corresponding gravity-wave drag anomaly [*Karlsson et al.*, 2009a, Figure 8] shows that the drag anomaly is absent equatorward of 20°N. This suggests the equatorial warming region present in the model is not related to a change in gravity-wave drag and that the temperature anomaly that straddles the equatorial mesosphere is due to a different process that abuts the region of anomalous gravity wave drag.

[43] It is noteworthy that there is observational [*Yulaeva et al.*, 1994] and modeling [*Semeniuk and Shepherd*, 2001] support for a planetary-wave driven (and seasonally varying) upwelling at the equator. However, the processes responsible for this upwelling differ to those at play at mid- and high-latitudes and respond differently to the perturbations triggered by interhemispheric coupling. As such, they appear in the mean atmospheric state but not the correlation analysis used here.

[44] The Coriolis effect plays a role in stage 3 of the BKK mechanism. *Karlsson et al.* [2009a] and *Körnich and Becker* [2010] note that a warm region in the low-latitude summer mesosphere will increase the local poleward temperature gradient. Thermal wind arguments suggest this will increase the subtropical zonal wind, weaken the summer westward flow (and affect its vertical shear) and affect gravity wave propagation and breaking. In the presence of this warm (cold) region, a vertical dipole in gravity-wave drag perturbation is expected with a decrease (increase) above an increase (decrease) in zonal-wave drag. This in turn creates a meridional and vertical circulation that displaces the meridional temperature gradient perturbation and allows it to propagate poleward and upward. However, the zonal wind response due to a meridional thermal gradient (as described in derivations of the thermal wind equation [see, e.g., *Andrews et al.*, 1987]) is also dependent on the Coriolis effect; this part of the BKK mechanism will also be ineffective near the equator.

[45] The propagation of such a temperature perturbation from near the equator to the summer pole is demonstrated in modeling results of *Karlsson et al.* [2009a, Figure 8] (however, the vertical gravity-wave drag dipole described above is, once again, weak near the summer side of the equator). Observational support also exists for stage 3 of the BKK mechanism. *Goldberg et al.* [2009] described the propagation of a temperature anomaly extracted from northern hemisphere SABER temperature observations taken during the 2002 stratospheric warming. This anomaly was seen to propagate from near the equator to the northern polar regions in a manner very similar to that described in *Karlsson et al.* [2009a]. The QBO was in its eastward phase at this time, making the latitudinal extent of the southern hemisphere planetary wavefield greater.

[46] The observations depicted in Figure 8 suggest a similarity of the response to both stage 1 and the polar part of stage 2 of the BKK mechanism between QBO phases. However, they differ from the proposed interhemispheric coupling mechanism in two ways. The temperature response near the equator to changes in planetary wave activity is absent or weak, and the winter midlatitude temperature response near 1 hPa is stronger for QBO westward (it being almost absent for QBO eastward).

[47] These points of difference potentially affect the initiation of stage 3 of the proposed mechanism and allow an explanation of the finding that the QBO reverses the sign of the interhemispheric coupling to the meridional wind at 86 km (Figure 1) to be proposed. In stage 3, a meridional and vertical wind anomaly (and its associated temperature perturbation) propagates upward and toward the summer polar mesosphere. In the westward phase of the QBO, this stage is likely initiated in the winter midlatitudes near 1–2 hPa. It is not possible to predict where it is initiated in the QBO eastward case from the data presented here but it will be at a different height and latitude to the QBO westward case. This difference in the starting point of the perturbation will mean the height at which the vertical wind anomaly reaches the summer pole will differ for the two QBO phases. As discussed in section 4.1, the zonal-mean meridional wind relates to the vertical wind and its vertical gradient. Both of these parameters are potentially affected by the height at which the vertical wind anomaly perturbs the summer polar vertical background wind. The relative perturbation of the vertical wind and its gradient will define the magnitude and sign of the response in the meridional wind.

[48] It has been noted that, due to the weakness of the Coriolis effect, the link between stages 2 and 3 of the BKK mechanism as it crosses the equator needs further explanation. This work is beyond the scope of this paper but could also contribute to the difference in response between QBO phases.

[49] Differences in the lag associated with the interhemispheric coupling for the two QBO phases (as shown in Figure 4) also suggest that the propagation path of the temperature anomaly to the summer mesosphere differs between QBO phases. The relative differences between the correlation patterns in Figure 8 remain the same when lags of up to −5 or −10 days are introduced. This suggests that the overall lag differences come about in stage 3 of the BKK mechanism (or its initiation).

[50] The dependence of the stage 3 temperature anomaly on the character of the gravity waves propagating up to it needs to be noted. The wave phase speed spectrum will affect the vertical drag dipole and the rate at which it propagates poleward and vertically. In turn, this will affect the character of interhemispheric coupling. Further attempts to

reconcile observations and modeling studies may be useful in tuning gravity-wave drag parameterization schemes.

5. Summary and Conclusion

[51] Radar observations of the high southern latitude MLT winds, when correlated with global UKMO assimilated temperature fields, illustrate another manifestation of the interhemispheric coupling described by *Becker and Fritts* [2006] and *Karlsson et al.* [2007, 2009b]. They also show that the QBO acts to vary the response in the meridional wind at 86 km. This modulating effect of the QBO is not accounted for in the BKK coupling mechanism, however, *Espy et al.* [2011] show that Holton-Tan induced stratospheric temperature variations [*Holton and Tan*, 1980] can modulate the first stage of the BKK mechanism and propagate a QBO signal to the northern mesopause.

[52] Investigations of the coupling using UKMO data provide support for the first two stages of the BKK mechanism but suggest the low-latitude branch of the winter gravity-wave drag driven dipole is absent for the QBO eastward case. They also suggest the temperature response to altered planetary-wave drag is weak in the vicinity of the equator. These points of difference between observations and the BKK mechanism provide a potential explanation for the QBO modulation of the MLT meridional wind response.

[53] Continuity and hydrostatic arguments show that the zonal-mean meridional wind near the poles is influenced by both the zonal-mean vertical wind and its vertical gradient. The QBO clearly influences both the height and latitude at which stage 3 of the BKK mechanism is initiated. These changes will also affect the height at which the stage 3 anomaly arrives at the pole and the resultant changes to the vertical wind profile. It should be noted that the temperature response in the summer mesosphere is likely more strongly coupled to the vertical wind anomaly than to changes in its gradient. It is therefore possible that the QBO affects interhemispheric coupling to the mesospheric temperature less than it does the meridional wind.

[54] Modeling studies so far have not included the potential influence of the QBO and other observational studies have not contained sufficient data to consider its effect in the manner applied here. The observations presented in this paper, and the role that winter hemisphere planetary waves play in the proposed mechanism for interhemispheric coupling show the importance of consideration of the QBO in future studies. The mechanism responsible for the propagation of the mesospheric temperature anomaly across the equator should also be the subject of further investigation. In particular, the role gravity-wave drag (or its parameterization in a model) may play in the formation and propagation of the anomaly should be considered.

Appendix A: Mass Continuity and the Relationship Between Meridional and Vertical Velocity

[55] Insight into mean atmospheric meridional and vertical motions in the presence of wave drag (as is the case in the MLT region) can be gained through the use of the "Downward Control" principle [*Haynes et al.*, 1991; *Garcia and Boville*, 1994]. This approach integrates the effect of wave drag above the level of interest. Unfortunately, the data of a quality required to invoke this principle in practice are often not available. A simpler approach is to use continuity arguments to relate the zonal-mean meridional velocity to the zonal-mean vertical velocity (and its gradient) for a given latitude and height. In this section, the continuity equation is used to explore the limits of these arguments.

[56] The zonally averaged mass-conservation equation in spherical coordinates [e.g., *McIntyre*, 1989] can be reduced to

$$\frac{\partial(\rho\overline{w})}{\partial z} = \frac{\rho(z_0)}{(a+z_0)}\left[\overline{v}\tan\varphi - \frac{\partial\overline{v}}{\partial\varphi}\right], \tag{A1}$$

where $\rho(z)$ is the density at a height z, φ is the latitude (negative for the southern hemisphere), $\overline{v}$ and $\overline{w}$ are the zonal-mean meridional and vertical velocities respectively, a is the radius of the earth and z_0 is the height of the region of interest.

[57] This is an expression for the contribution made to the vertical mass flux $\rho\overline{w}$ over a height range dz around z by the zonal-mean meridional flow. The two terms in this equation reflect the contribution made by the convergence of lines of longitude and by the meridional shear of meridional velocity. The importance of the former is weighted by the latitude through the $\tan\varphi$ term and becomes greater than unity poleward of 45°. The latter term accounts for changes in zonal-mean meridional velocity as a function of latitude as these too must have an associated vertical mass flux.

[58] It is necessary for the zonal-mean meridional velocity to equal zero at the pole to avoid a discontinuity in $\partial\overline{v}/\partial\varphi$ at that point. To remain consistent with this while allowing for non-zero zonal-mean meridional velocities away from the pole, it is assumed that $\overline{v}$ varies linearly with co-latitude (at high latitudes) and is zero at the pole. The latitudinal gradient of the meridional wind is then simply related to the amplitude of the wind at a given latitude. The two terms in equation (A1) reduce to a constant factor times the zonal-mean meridional velocity. For the latitude of Davis, the gradient of vertical mass flux is given by

$$\frac{\partial(\rho\overline{w})}{\partial z} = -5.23.\overline{v}\frac{\rho(z_0)}{(a+z_0)}. \tag{A2}$$

[59] The expression on the left hand side of this equation can be expanded as

$$\begin{aligned}\frac{\partial(\rho\overline{w})}{\partial z} &= \overline{w}\frac{\partial\rho}{\partial z} + \rho\frac{\partial\overline{w}}{\partial z} \\ &= -\frac{\rho}{H}\overline{w} + \rho\frac{\partial\overline{w}}{\partial z}\end{aligned} \tag{A3}$$

where it is assumed that the density decays exponentially with height at a rate given by $\rho(z) = \rho_0 \exp(-z/H)$, ρ_0 a reference density and H the density scale height.

[60] Combining equations (A2) and (A3) gives

$$K\overline{v} = \frac{\overline{w}}{H} - \frac{\partial\overline{w}}{\partial z}, \tag{A4}$$

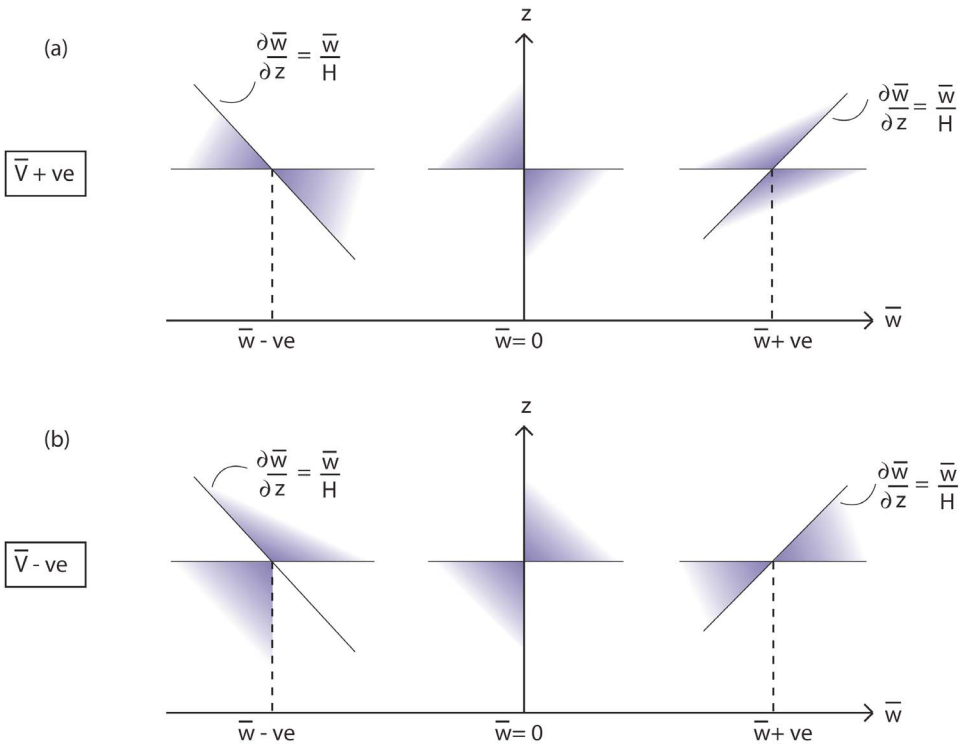

Figure A1. Allowed ranges (shaded) of $\partial\overline{w}/\partial z$ for $\overline{v}$ (a) positive and (b) negative and for $\overline{w}$ positive, zero and negative at high southern latitudes. Straight lines describing the slope of the vertical velocity must overlie the shaded regions.

where $K = 5.23/(z_0 + a)$ combines the constant and the height into a single (positive) quantity.

[61] This equation shows that, when the zonal-mean form of the continuity equation is coupled to the density expected in a hydrostatic atmosphere, the meridional velocity at z_0 defines a combination of *both* the vertical velocity and its variation with height. The consequences of this result are explored by considering the inequalities that arise from equation (A4) for cases of positive and negative meridional velocity:

$$\text{Positive } \overline{v} : K\overline{v} > 0 \Rightarrow \frac{\partial \overline{w}}{\partial z} < \frac{\overline{w}}{H} \tag{A5}$$

$$\text{Negative } \overline{v} : K\overline{v} < 0 \Rightarrow \frac{\partial \overline{w}}{\partial z} > \frac{\overline{w}}{H}. \tag{A6}$$

[62] In Figure A1a, the ranges of $\partial\overline{w}/\partial z$ that are consistent with positive values of zonal-mean meridional velocity (and the assumptions described above) are presented for a range of $\overline{w}$ values (represented on the horizontal axis). The limiting slopes are infinity and $\overline{w}/H$ with the latter varying according to the value and sign of $\overline{w}$. On the left hand side of Figure A1a (and on the axis), only negative $\partial\overline{w}/\partial z$ cases (or negative plus zero cases) are possible. On the right hand side of this panel ($\overline{w}$ positive) both positive and negative $\partial\overline{w}/\partial z$ provide a broader range of options. In Figure A1b, the case for negative meridional velocity is illustrated. In contrast to the previous case, it is the negative $\overline{w}$ values that provide a broader range of background vertical wind conditions that are consistent with continuity and hydrostatic balance.

[63] It is noted that the arguments presented here are for a single height and so do not constrain the rate of change of $\overline{w}$ with height. Continuity and the requirement for hydrostatic balance must apply at all points in the wind field but neither provide any constraints on this slope. It is the vertical structure of dynamical processes such as gravity waves breaking that will define the height variation of the wind field. However, the above arguments show that, in the southern polar regions, positive values of $\overline{v}$ are less constrained when $\overline{w}$ is positive; continuity is satisfied more easily when both $\overline{v}$ and $\overline{w}$ are positive. Thus positive values of $\overline{w}$ are likely to be associated with positive values of $\overline{v}$. Similarly, negative values of $\overline{w}$ are likely to be associated with negative values of $\overline{v}$.

[64] A standard construct of upwelling over the pole being associated with positive (in the southern hemisphere) values of zonal-mean meridional velocity in the 'outflow' region of the upper mesosphere/lower thermosphere is consistent with the above arguments. However, more than continuity arguments are needed to support the construct; the vertical structure of the wind field, or the dynamical processes on which it depends, need to be defined [see, e.g., *Fritts and Luo*, 1995].

[65] **Acknowledgments.** Operational and research activities associated with the Davis MF radar have been supported by Australian Antarctic Science Advisory Committee grant 674 and Australian Research Council grant DP0346394. The authors are grateful for the efforts of the many engineers that have supported the operation of the radar at Davis since its installation. The technical support provided by Atmospheric Radar Systems is

also acknowledged. The thoughtful comments of the three reviewers have helped to improve this manuscript and we thank them for their contribution.

References

Andrews, D. G., J. R. Holton, and C. B. Leovy (1987), *Middle Atmosphere Dynamics*, Academic, San Diego, Calif.

Baldwin, M. P., et al. (2001), The quasi-biennial oscillation, *Rev. Geophys.*, *39*(2), 179–229, doi:10.1029/1999RG000073.

Baldwin, M., T. Hirooka, A. O'Neill, and S. Yoden (2003), Major stratospheric warming in the southern hemisphere in 2002: Dynamical aspects of the ozone hole split, *SPARC Newsl.*, *20*, 24–26.

Becker, E., and D. C. Fritts (2006), Enhanced gravity-wave activity and interhemispheric coupling during the MaCWAVE/MIDAS northern summer program 2002, *Ann. Geophys.*, *24*, 1175–1188.

Becker, E., and G. Schmitz (2003), Climatological effects of orography and land-sea heating contrasts on the gravity wave-driven circulation of the mesosphere, *J. Atmos. Sci.*, *60*, 103–118.

Becker, E., A. Müllemann, F.-J. Lübken, H. Körnich, P. Hoffmann, and M. Rapp (2004), High Rossby-wave activity in austral winter 2002: Modulation of the general circulation of the MLT during the MaCWAVE/MIDAS northern summer program, *Geophys. Res. Lett.*, *31*, L24S03, doi:10.1029/2004GL019615.

Dunkerton, T. (1978), On the mean meridional mass motions of the stratosphere and mesosphere, *J. Atmos. Sci.*, *35*, 2325–2333.

Espy, P. J., S. O. Fernández, P. Forkman, D. Murtagh, and J. Stegman (2011), The role of the QBO in the inter-hemispheric coupling of summer mesospheric temperatures, *Atmos. Chem. Phys.*, *11*, 495–502, doi:10.5194/acp-11-495-2011.

Fritts, D. C., and Z. Luo (1995), Dynamical and radiative forcing of the summer mesopause circulation and thermal structure: 1. Mean solstice conditions, *J. Geophys. Res.*, *100*(D2), 3119–3128.

Garcia, R. R., and B. A. Boville (1994), "Downward control" of the mean meridional circulation and temperature distribution of the polar winter stratosphere, *J. Atmos. Sci.*, *51*(15), 2238–2245.

Geller, M. A. (1983), Dynamics of the middle atmosphere, *Space Sci. Rev.*, *34*, 359–375.

Goldberg, R. A., A. Feofilov, A. Kutepov, F. J. Schmidlin, and J. M. Russell (2009), Evidence for interhemispheric coupling during the unusual northern polar summer mesosphere of 2002, *Eos Trans. AGU*, *90*(52), Fall Meet. Suppl., Abstract SA33B-06.

Haynes, P. H., C. J. Marks, M. E. McIntyre, T. G. Shepherd, and K. P. Shine (1991), On the "Downward control" of extratropical diabatic circulations by eddy-induced mean zonal forces, *J. Atmos. Sci.*, *48*(4), 651–678.

Holton, J. R., and H.-C. Tan (1980), The influence of the equatorial quasi-biennial oscillation on the general circulation at 50 mb, *J. Atmos. Sci.*, *37*, 2200–2208.

Karlsson, B., H. Körnich, and J. Gumbel (2007), Evidence for interhemispheric stratosphere-mesosphere coupling derived from noctilucent cloud properties, *Geophys. Res. Lett.*, *34*, L16806, doi:10.1029/2007GL030282.

Karlsson, B., C. McLandress, and T. G. Shepherd (2009a), Inter-hemispheric mesospheric coupling in a comprehensive middle atmosphere model, *J. Atmos. Sol. Terr. Phys.*, *71*, 518–530, doi:10.1016/j.jastp.2008.08.006.

Karlsson, B., C. E. Randall, S. Benze, M. Mills, V. L. Harvey, S. M. Bailey, and J. M. Russell III (2009b), Intra-seasonal variability of polar mesospheric clouds due to inter-hemispheric coupling, *Geophys. Res. Lett.*, *36*, L20802, doi:10.1029/2009GL040348.

Körnich, H., and E. Becker (2010), A simple model for the interhemispheric coupling of the middle atmosphere circulation, *Adv. Space Res.*, *45*(5), 661–668, doi:10.1016/j.asr.2009.11.001.

Lindzen, R. S. (1981), Turbulence and stress owing to gravity wave and tidal breakdown, *J. Geophys. Res.*, *86*, 9707–9714.

McIntyre, M. E. (1989), On dynamics and transport near the polar mesopause in summer, *J. Geophys. Res.*, *94*(D12), 14,617–14,628.

Murphy, D. J. (1984), Vertical motions in the mesosphere, Master's thesis, Univ. of Adelaide, Adelaide, South Aust., Australia.

Murphy, D. J., W. J. R. French, and R. A. Vincent (2007), Long-period planetary waves in the mesosphere and lower thermosphere above Davis, Antarctica, *J. Atmos. Sol. Terr. Phys.*, *69*, 2118–2138, doi:10.1016/j.jastp.2007.06.008.

Randel, W. J. (1993), Global variations of zonal mean ozone during stratospheric warming events, *J. Atmos. Sci.*, *50*(19), 3308–3321.

Semeniuk, K., and T. G. Shepherd (2001), Mechanisms for tropical upwelling in the stratosphere, *J. Atmos. Sci.*, *58*, 3097–3115.

Yulaeva, E., J. R. Holton, and J. M. Wallace (1994), On the cause of the annual cycle in tropical lower-stratospheric temperatures, *J. Atmos. Sci.*, *51*(2), 169–174.